

# Change of electrochemical impedance spectra (EIS) with time during CO-poisoning of the Pt-anode in a membrane fuel cell

N. Wagner\*, E. Gülzow

*Deutsches Zentrum für Luft- und Raumfahrt (DLR), Institut für Technische Thermodynamik, Pfaffenwaldring 38-40, D-70569 Stuttgart, Germany*

## Abstract

This paper focuses on the electrochemical characterisation, e.g. current-voltage-measurement and time resolved electrochemical impedance spectroscopy (TREIS) of polymer electrolyte fuel cells (PEFCs) during operation of the fuel cell with oxygen and  $H_2 + 100$  ppm CO respectively. Due to the poisoning effect of carbon monoxide, the system changes its state during the experiment. The reconstruction of quasi-causal impedance spectra was made by using enhanced numerical procedures. The reconstructed impedance spectra recorded at constant load, in galvanostatic mode of operation of the fuel cell show a strong time dependence and exhibit pseudo-inductive contributions at the low frequency part of the spectra which increase during the experiment. The analysis of the spectra suggests that the pseudo-inductive behaviour can be attributed to a surface relaxation process of the anode. Furthermore, the influence of the carbon monoxide on the electrochemical behaviour of the contaminated fuel cell may be interpreted by means of a Faraday impedance in addition with a potential-dependent hindrance of the charge transfer.

Otherwise, the impedance spectra recorded during CO poisoning of the anode at constant cell voltage, in the potentiostatic mode of operation of the fuel cell, show also a strong time dependence, but no pseudo-inductive contribution in the low frequency part of the spectra. © 2003 Elsevier B.V. All rights reserved.

**Keywords:** Polymer electrolyte fuel cells (PEFCs); Carbon monoxide poisoning; Time resolved electrochemical impedance spectroscopy (TREIS); Surface relaxation; Porous electrode model

## 1. Introduction

Due to the high energy conversion rate and emission free-operation, polymer electrolyte fuel cells (PEFCs) have been receiving more and more attention for powering electric vehicles. The highest performance is achieved with pure hydrogen ( $H_2$ ) which is the preferred fuel for low-temperature fuel cells [1,2].

However, pure  $H_2$  has several limitations. First of all, the storage systems for liquid or compressed  $H_2$  are heavy and bulky. Furthermore,  $H_2$  refueling is costly and takes time. An alternative solution is the in situ generation of hydrogen on board of the electric vehicle by reforming either hydrocarbons (e.g. natural gas, biogas) or alcohol's (e.g. methanol, ethanol). The reformate feed gas may contain up to 2.5% carbon monoxide (CO) by volume, which can be reduced to about 50 ppm CO using a selective oxidiser [3].

The performance of platinum which is known as one of the most effective catalysts for the hydrogen oxidation in polymer membrane fuel cells is influenced even by traces

of carbon monoxide: compared with the use of pure hydrogen, the maximum power density is more than halved in the presence of only 5 ppm carbon monoxide [4]. One possible explanation for the decrease of the fuel cell performance is that the carbon monoxide blocks or limits the active sites of the platinum catalyst due to adsorption which leads to an inhibition of the hydrogen oxidation reaction [5–8].

For the development of improved catalysts which are less sensitive with respect to the presence of carbon monoxide, a mechanistic understanding of the poisoning process of the anode is desirable. The progressive poisoning with carbon monoxide of a fuel cell was monitored using time resolved electrochemical impedance spectroscopy (TREIS). Therefore, measurement at distinct time intervals during the experiment were performed. The poisoning causes a change of the state of the fuel cell which is reflected in the recorded impedance spectra. Besides, an increase of the total impedance of the fuel cell, in the case of galvanostatic mode of operation, the occurrence and the increase of a pseudo-inductive behaviour is observed [9]. For the evaluation of the series measurement's, enhanced mathematical procedures, like the real-time drift compensation [10,11], the time course interpolation [12,13], and an additional refinement were applied to reduce the influence of the changing

\* Corresponding author. Tel.: +49-711-6862-631;  
fax: +49-711-6862-322.  
E-mail address: [norbert.wagner@dlr.de](mailto:norbert.wagner@dlr.de) (N. Wagner).

state of the fuel cell in the obtained spectra. Due to the experimental conditions, in the case of galvanostatic mode of operation, the evaluation of the spectra can be considerably simplified.

## 2. Experimental

The impedance measurements were carried out in a 23 cm<sup>2</sup> single cell (Fig. 1) with stainless steel sinter plates having a porosity of 50% as the gas distribution structure [14]. The membrane electrode assembly (MEA) consisted of two electrodes with 20 wt.% Pt/C (purchased from E-TEK), hot pressed (1.6 MPa, 10 min, increasing temperature up to 160 °C) onto a proton exchange membrane (Nafion 117, purchased from DuPont).

The cells were run at 80 °C. Pure hydrogen or hydrogen with addition of 100 ppm carbon monoxide were used as the anodic fuel and oxygen as the cathodic gas, both gases at 2 bar absolute pressure. The hydrogen/carbon monoxide mixture flowed ‘dead end’ (the anodic gas outlet was closed) whereas the amount of oxygen was adjusted to the applied current densities, exceeding up to eight times the stoichiometric requirement for the applied current. The influence of the carbon monoxide poisoning was investigated by means of EIS. The electrochemical impedance measurements were performed using a Zahner IM6 workstation in addition with an external current sink EL100 under a constant load of 5 A ( $\cong 217 \text{ mA cm}^{-2}$ ) within a frequency range between 10 kHz and 0.050 Hz. A series of measurements at periodic time intervals was recorded during the experiment applying a small sine-wave distortion of 200 mA amplitude. A twisted-pair

arrangement of the current as well as of the sensing lines was used to depress the mutual induction effect which is often observed in the high frequency region of impedance measurements at low-ohmic systems [15].

In addition to the impedance spectra recorded during constant load of the fuel cell, a series of time-dependent impedance spectra at constant cell voltage (700 mV) were recorded, in the potentiostatic mode of fuel cell operation. In this case, a small sine-wave distortion (AC signal) of 10 mV amplitude was applied.

## 3. Results and model discussion

### 3.1. Measurements at constant cell voltage

First measurements performed with H<sub>2</sub>/100 ppm CO have been carried out in the potentiostatic mode of fuel cell operation at constant cell voltage. The cell voltage was kept constant at 700 mV. After changing the anode feed gas from pure H<sub>2</sub> to H<sub>2</sub>/100 ppm CO, one can observe (Fig. 2) three different sections: a nonlinear decrease of the current density immediately after adding 100 ppm CO to the hydrogen feed gas ( $t = 0$ ;  $i = 268 \text{ mA cm}^{-2}$ ), a transition behaviour between 250 and 100 mA cm<sup>-2</sup> and finally a slow current density decay. At each point of the  $i = f(t)$  curve of Fig. 2 an impedance spectrum was recorded (Fig. 3). The impedance spectra, represented as Nyquist plots, were obtained by varying the frequency of the voltage perturbation signal from 0.05 Hz to 20 kHz in order to get more information in the poisoning period. One of the prerequisites of impedance measurements is a quasi-steady state of the

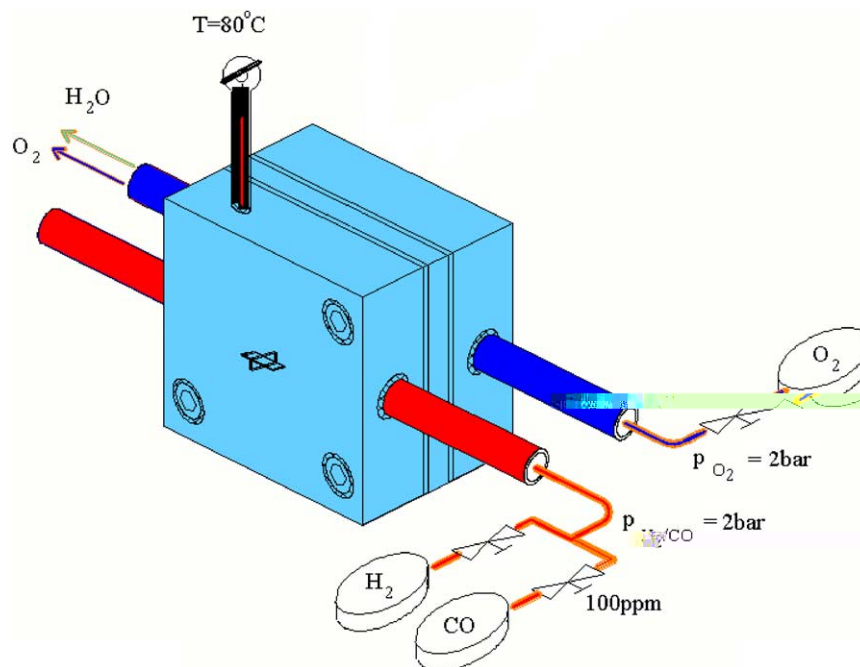


Fig. 1. Schematic view of the experimental set-up used for electrochemical measurement.

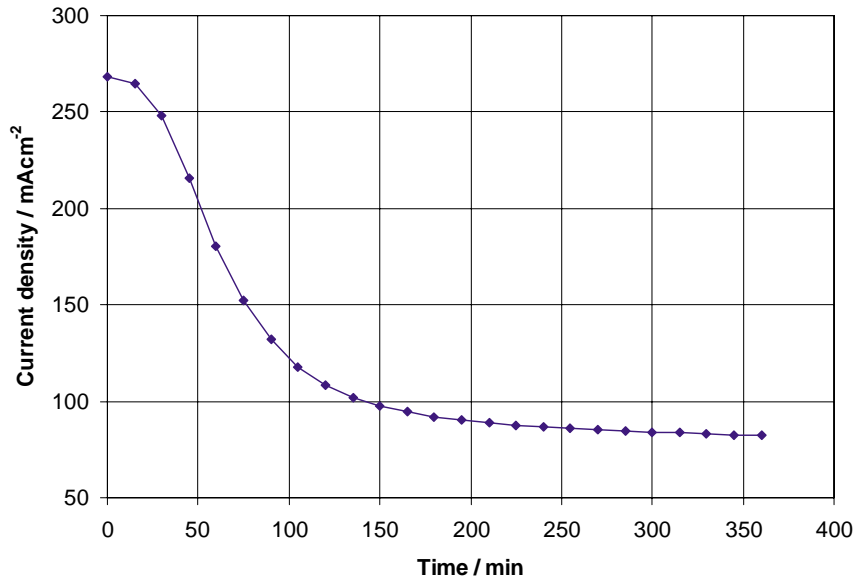


Fig. 2. Time progression of current density during potentiostatic mode of operation at a cell voltage of 700 mV with H<sub>2</sub> + 100 ppm CO at 80 °C.

system under investigation. Thus, recording of impedance spectra of a system which alters its electrochemical state leads to the possibility that at each frequency a significantly differing current density is present. Provided that the time for acquisition is available for each frequency sample, data

can be transformed by interpolation to generate impedance spectra which belong to well defined times.

Since the current density changed during the impedance measurements, the cell impedance also changed with time. The cell impedance can be attributed to the membrane

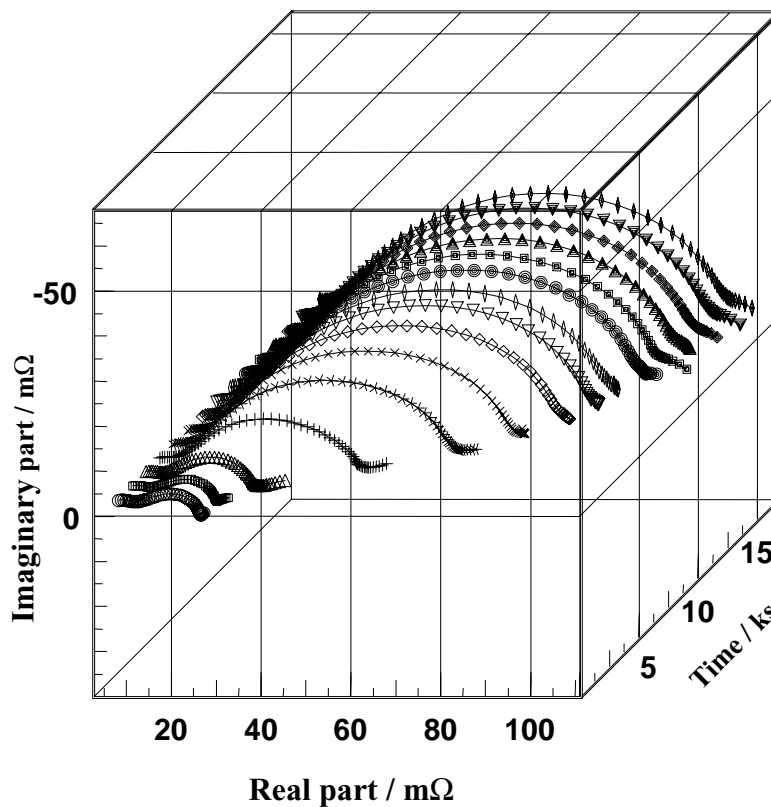


Fig. 3. Nyquist plots of the interpolated impedance spectra measured at 700 mV and different times during progressive poisoning of the anode with CO.

resistance and the current density-dependent impedance of the anode and cathode respectively. Both, the impedances of anode and of the cathode change with time (current density), so that the evaluation of the impedance spectra at constant cell voltage during poisoning of the anode is difficult. To avoid the simultaneous change of both contributions to the cell impedance, the impedance measurements were performed in the galvanostatic mode of fuel cell operation.

### 3.2. Measurements at constant current density

The electrochemical impedance measurements were carried out in galvanostatic mode. All impedance spectra reported herein were measured between the fuel cell cathode and anode. In the galvanostatic mode with a constant current (5 A or  $217 \text{ mA cm}^{-2}$ ), the impedance of the cathode and the membrane resistance can be assumed to be constant and the changes in the impedance spectra during poisoning the anode with CO can be attributed exclusively to the impedance of the anode. The current and the potential were each collected with two interwired circuit cables. At each potential value, a small AC perturbation (200 mA amplitude) was applied between the anode and the cathode of the FC.

Similar to the measurements at constant cell voltage, also the cell voltage changed during progressive CO poisoning

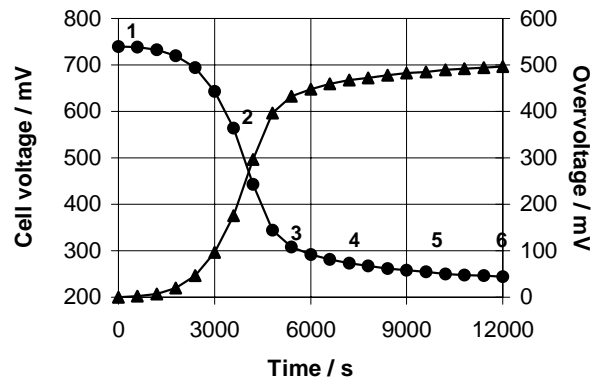


Fig. 4. Time progression of cell voltage and overvoltage during galvanostatic mode of operation of the fuel cell at  $217 \text{ mA cm}^{-2}$  with  $\text{H}_2 + 100 \text{ ppm CO}$  at  $80^\circ\text{C}$ .

of the anode at constant current density (Fig. 4). Representative impedance measurements of the series are depicted in Fig. 5 as Nyquist plots. At the beginning of the experiment, one recognises a full, depressed (capacitive) semicircle in addition to an onset of a second semicircle at low frequencies. With increasing time, the real as well as the imaginary part of the impedance increase and the two semicircles are no longer resolvable visually. In addition, the fuel cell impedance exhibits an enlarged pseudo-inductive behaviour

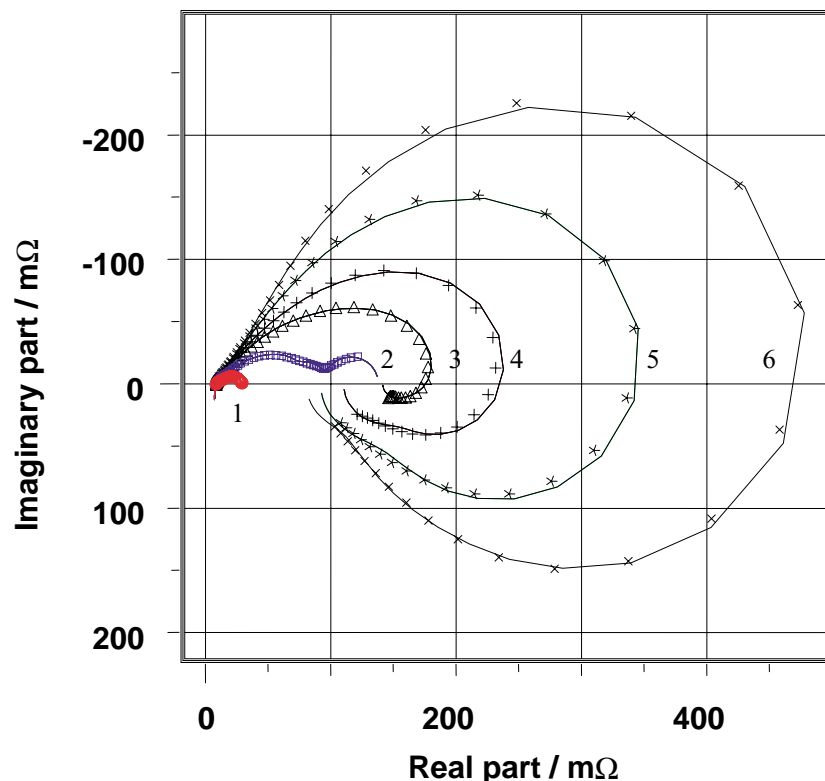


Fig. 5. Nyquist plots of the fuel cell impedance at different times; the influence of the carbon monoxide poisoning leads to an increase of both the real and imaginary part of the impedance during the experiment; at the beginning (left part of the diagram) the anodic and cathodic impedances are separable (two half cycles in the Nyquist plots); with increasing time, the anodic cell impedance increases and becomes more and more dominant, 'hides' the cathodic cell impedance and exhibits an enlarged pseudo-inductive behaviour.

at the low frequency side with increasing time. At the end of the experiment, the impedance spectrum resembles more a full circle than a semicircle which is observed at the beginning of the experiment.

As expected from the previous impedance measurements at constant cell voltage, the evolution of the impedance spectra indicate that the carbon monoxide poisoning causes a change of the state of the system under investigation. One has to assume that the system changes its state not only between two measurements but also during the recording of a single spectrum. The latter fact causes problems for the evaluation of the spectrum, because the recording of an impedance spectrum one frequency after each other requires a finite time, while the measurement at high frequencies requires less time than the measurement at low frequencies. Due to the fact that the recording of a single spectrum in the frequency range mentioned above requires about 20 min, the influence of the changing state to the measured spectrum is not negligible. For this reason, one of the fundamental prerequisites for the evaluation of impedance measurements is violated. Nevertheless it is possible, as in the case of measurements at constant cell voltage, to reconstruct ‘quasi steady state’ (and therefore ‘quasi causal’) spectra from drift affected impedance data using enhanced mathematical procedures, provided that the time of acquisition is available for each frequency sample.

As recently shown [16–20], a combination of three mathematical procedures can be applied successfully for the interpretation of impedance measurements of fuel cells which exhibit non-steady state behaviour. These techniques are denoted as the real-time drift compensation, the time course interpolation and finally the Z-HIT refinement.

As reported in recent papers [21,22], the separation of the contributions of the anode from these of the cathode is the main problem for the analysis of the impedance spectra of the fuel cell. Both half cells consist of a porous system separated by the membrane. Therefore, in principle, the half cell impedances should be modelled using the same elements, like a porous electrode and a (finite) diffusion impedance. The results presented here are based on a more general concept for the improvement of fuel cells by means of EIS. This concept requires that the experimental conditions for a distinct investigation are modified, so that a simplification of the equivalent circuit for the interpretation of the obtained impedance spectra is rendered possible. First of all, in galvanostatic mode of operation the current density remains constant at the electrodes. In contrast to the potentiostatic mode of operation, the evaluation of the charge transfer resistances is facilitated, because the values are inversely proportional to the exchange current density. At the same time, the galvanostatic mode forces a constant conversion rate with respect to the (charged) species which are involved in the electrode reactions.

Due to these experimental conditions it is assumed that the alterations in the impedance spectra are dominated by the shift of the anodic half cell reaction. Therefore, the

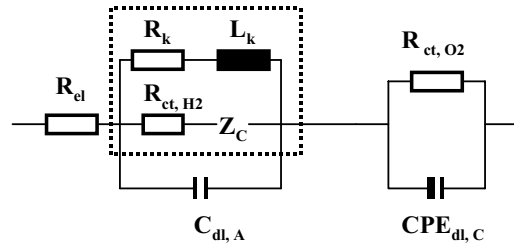


Fig. 6. Equivalent circuit for evaluation of the interpolated impedance spectra measured in galvanostatic mode of operation of the fuel cell during poisoning the anode with CO.

effect of the progressive poisoning with carbon monoxide of the fuel cell can be described quantitatively according to the simplified model given in Fig. 6. In series to both half cells, the resistance of the membrane itself—denoted as the electrolyte resistance ( $R_{el}$ )—as well as a parasitic inductance due to the mutual induction effect has to be taken into account. The impedance of the cathodic half cell (oxygen reduction) is approximated using a charge transfer resistance ( $R_{ct,O_2}$ ) in parallel to a constant phase element (CPE). This simple equivalent circuit describes the partial impedance contribution of the cathodic half cell with sufficient accuracy. For this reason, an accurate description of the physico-chemical model of the cathode—besides its impedance—is neither intended nor necessary.

In contrast, the impedance of the anodic part (hydrogen oxidation) is more complex due to processes within the pores of the anode which are influenced by the carbon monoxide poisoning. The anodic impedance is modelled using a porous electrode [23]. The impedance of the interface electrode/pore is given by the double layer capacity ( $C_d$ ) which is in parallel to the Faraday impedance  $Z_F$ . The Faraday impedance is a surface relaxation impedance [24,25]. The relaxation impedance explains the development of the pseudo-inductive behaviour in the low frequency range of the impedance spectra of the fuel cell. The surface relaxation impedance represents a Faraday impedance at non-equilibrium potential with a potential-dependent transfer reaction rate ( $k$ ) and its time-dependent relaxation according to Eq. (1) [26].

$$Z_F = \frac{R_{ct} + Z_C}{1 + R_{ct}/Z_K} \quad (1)$$

$$Z_K = \frac{1 + j\omega\tau_K}{I_F d(\ln k)/d\varepsilon} \quad \text{with} \quad R_K = \frac{1}{I_F d(\ln k)/d\varepsilon} \quad \text{and} \quad X_K = j\omega\tau_K R_K = j\omega L_K \quad (2)$$

In Eq. (1),  $R_{ct}$  denotes the charge transfer resistance of the anode ( $R_{ct,H_2}$  in Fig. 6),  $Z_K$  is defined as the relaxation impedance according to Eq. (2), where  $I_F$  denotes the Faraday current,  $\tau_K$  the time constant of relaxation and the expression  $d(\ln k)/d\varepsilon$  is the first derivative of the logarithm of the reciprocal relaxation time constant against the potential  $\varepsilon$ . According to its frequency dependence,  $Z_K$  can be split into the relaxation-resistance  $R_K$  and the relaxation inductivity  $X_K$ , with the pseudo-inductance  $L_K = \tau_K R_K$  which

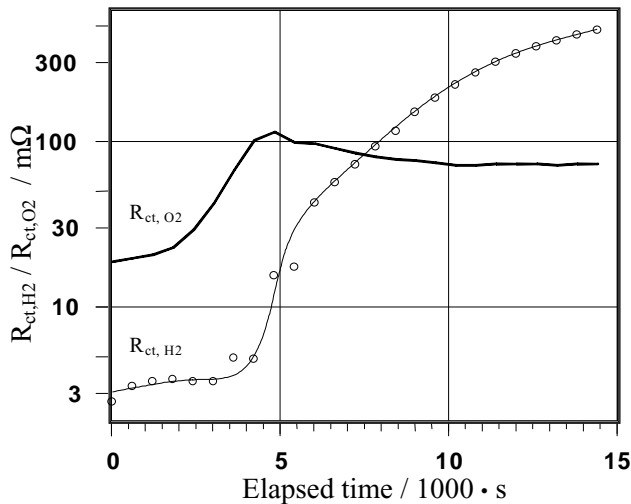


Fig. 7. Evolution of the cathodic charge transfer resistance  $R_{ct,O_2}$  (—), the anodic charge transfer resistance  $R_{ct,H_2}$  (○) for  $I = \text{constant} = 217 \text{ mA cm}^{-2}$  as a function of time.

is proportional to the relaxation time constant  $\tau_K$ . At least, for the finite diffusion impedance  $Z_C$  in Fig. 6, the well known Nernst impedance was chosen for the evaluation of the impedance spectra.

On the basis of this model, the alterations of the impedance spectra during the experiment are dominated by the changes of the charge transfer resistance (mainly  $R_{ct,H_2}$ ) and the surface relaxation impedance ( $R_K$ ,  $\tau_K$ ). The evolution of the charge transfer resistances ( $R_{ct,H_2}$  and  $R_{ct,O_2}$ ) are depicted in Fig. 7 as a function of the elapsed time (1 ks = 1000 s). It can be recognised that the cathodic charge transfer resistance ( $R_{ct,O_2}$ , —) increases from an initial value of 20  $m\Omega$  to a value of 120  $m\Omega$  at 5000 s and converges towards a constant value of about 88  $m\Omega$  at the end of the experiment. Therefore, the overall change is only about a factor of 4. In a first approximation, one would expect that the cathodic charge transfer resistance should remain constant during the experiment. However, it has to be taken into account that the effective charge transfer reaction is influenced by the concentrations of the charged as well as of the uncharged species (water). Moreover, the volume of the fuel cell is very small and therefore, the system is far away from a ‘thermodynamically ideal’ behaviour. Considering these two aspects it can be supposed that the poisoning of the anode side causes a local, inhomogeneous distribution of the generated protons and hence a inhomogeneous distribution of the protonated and associated water molecules at the anode side including the membrane. It is safe to assume that this inhomogeneous distribution causes also a local, inhomogeneous distribution of these species at the cathode side. From this point of view, it seems not to be surprising that the alterations at the anode side influence also an alteration of the charge transfer resistance at the cathode side. Comparing the alteration of the cathodic charge transfer resistance ( $dR_{ct,O_2}/dt$ ) with that of the anodic charge transfer resistance ( $dR_{ct,H_2}/dt$ ), one can denote the

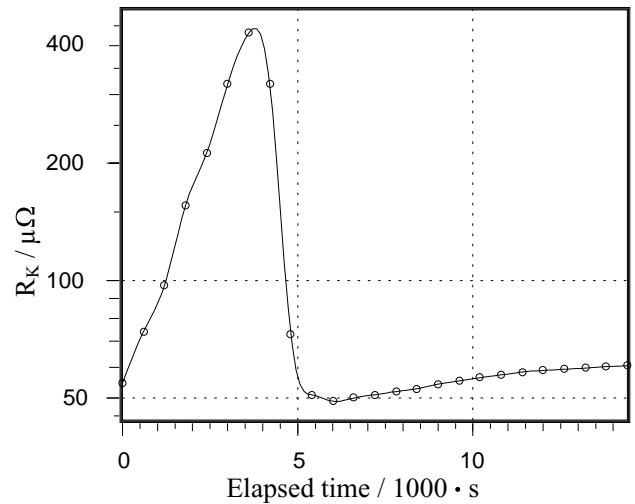


Fig. 8. Evolution of the anodic relaxation resistance  $R_K$  during progressive carbon monoxide poisoning.

alteration of the former to be small. The value of the charge transfer resistance of the anodic half cell reaction (Fig. 7;  $R_{ct,H_2}$ , ○) increases more than 2 orders of magnitude from 3 to 500  $m\Omega$ . The by far smaller alteration of the cathodic charge transfer resistance suggests that the (absolute) value of the cathodic potential can be considered to be almost constant during the whole experiment, as intended when choosing the experimental conditions of the measurements.

The effect of a continuous carbon monoxide poisoning during the experiment can be represented in the best way by plotting the resistance of relaxation  $R_K$  (Fig. 8) and the relaxation time constant (Fig. 9) as a function of time. Proceeding on the assumption that the potential of the cathodic half cell remains constant, the evolution of  $R_K$  can be explained as follows:

At the initial state of the experiment, the carbon monoxide begins to block active sites of the catalyst which causes a

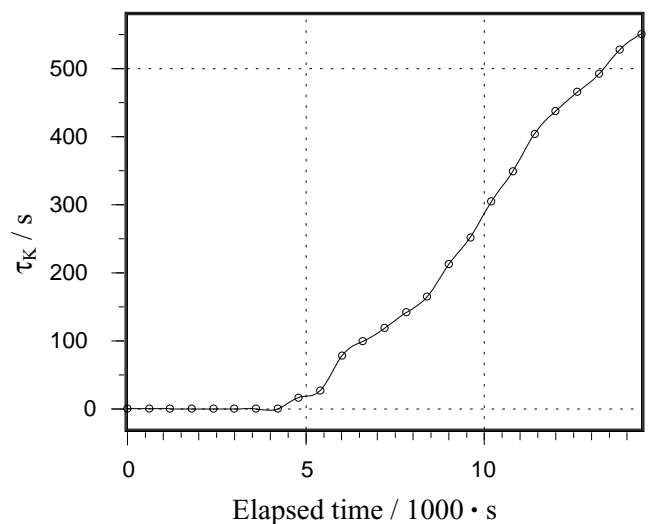


Fig. 9. Evolution of the anodic relaxation time constant  $\tau_K$  during progressive carbon monoxide poisoning.

decrease of the cell-voltage. As a consequence,  $R_K$  increases due to the term  $d(\ln k)/d\varepsilon$  in the denominator of Eq. (2). Simultaneously, the potential  $\varepsilon$  of the anodic electrode shifts towards that of the cathodic potential and therefore to more positive values, until the potential reaches a level, where the oxidation of carbon monoxide at Pt [27] is possible (about  $1\text{ h} = 3600\text{ s}$ ). Now, the oxidation of carbon monoxide to carbon dioxide, followed by a desorption of  $\text{CO}_2$ , leads to a 'reactivation' of the blocked (poisoned) catalyst and therefore, it becomes responsible for the decrease of  $R_K$ . From a chemical point of view, this reaction-sequence, the adsorption of carbon monoxide, oxidation at the Pt catalyst which requires the diffusion of water molecules to the adsorbed carbon monoxide and a final desorption of the generated carbon dioxide, is in competition with the 'normal' oxidation of hydrogen which also requires the presence of water for the desorption of the generated  $\text{H}^+$ -ions. From a more mechanistic point of view, this sequence causes a periodical change of the coverage of the electrode surface, inducing the potential oscillation observed.

In total, the resulting increase of the relaxation time constant  $\tau_K$  (Fig. 9) at times  $>5\text{ ks}$  is responsible for the increasing pseudo-inductive contributions which is observed in the impedance spectra of Fig. 5.

#### 4. Conclusion

During CO poisoning of the anode at constant cell voltage the current density decreases due to the blocking of the catalyst surface. Simultaneously, the cell impedance increases due to an increase of both impedance contributions: the anodic and cathodic impedance. By changing the experimental conditions, from constant cell voltage to constant load (current density) the change of the cell impedance is given mainly by the impedance of the anode. The value of the charge transfer resistance of the anodic half cell reaction increases more than 2 orders of magnitude from 3 to  $500\text{ m}\Omega$ . The by far smaller alteration of the cathodic charge transfer resistance suggests that the (absolute) value of the cathodic potential can be considered to be almost constant during the whole experiment, as intended when choosing the experimental conditions of the measurements.

During CO poisoning of the anode at constant current (5 A) the time course of the charge transfer resistances shows that the degradation of the fuel cell performance is dominated by an increase of the anodic resistance from 3 to  $500\text{ m}\Omega$ , whereas the cathodic one can be considered to be nearly constant during the whole experiment. The increasing pseudo-inductive behaviour can be explained by means of a surface relaxation process due to the competitive oxidation of hydrogen and carbon monoxide at the anode.

Impedance spectra measured during poisoning of the anode with CO show a strong time- and a potential-dependency, respectively. The most sensitive impedance elements are  $R_K$ ,  $\tau_K$  (increases from 0 to 550 ms) and the

reaction resistance of the hydrogen oxidation reaction  $R_{\eta}$  ( $R_{\text{ct},\text{H}_2}$ ) increases from 3 to  $500\text{ m}\Omega$ .

The fuel cell was operated in the "dead end" mode and the concentration of inert  $\text{CO}_2$  in the anode gas increased. The equivalent circuit proposed here can be extended by the porous electrode model and has to be verified by further impedance measurements under different operation conditions like different CO concentration, pressure, temperature and stoichiometry.

#### References

- [1] C. Borroni-Bird, J. Power Sources 61 (1996) 33.
- [2] S.J.C. Cleghorn, T.E. Springer, M.S. Wilson, C. Zawodzinski, T.A. Zawodzinski, S. Gottesfeld, Int. J. Hydrogen Energy 22 (1997) 1137.
- [3] D.P. Wilkinson, D. Thompsett, in: O. Savadogo, P.R. Roberge (Eds.), Proceedings of the Second National Symposium on New Materials for Fuel Cell and Modern Battery Systems, Montreal, Que., Canada, 1997, p. 268.
- [4] M.S. Wilson, C. Derouin, J. Valerio, T.A. Zawodzinski, S. Gottesfeld, Electrocatalysis, Issues in Polymer Electrolyte Fuel Cells. In: Proceedings of the 28th IECEC, 1993, pp. 1.1203–1.1208.
- [5] P. Stonehart, P.N. Ross, Catal. Rev. Sci. Eng. 12 (1975) 1.
- [6] M. Ciureanu, H. Wang, J. New Mater. Electrochem. Syst. 3 (2000) 107.
- [7] J.-D. Kim, Y.-I. Park, K. Kobayashi, M. Nagai, J. Power Sources 103 (2001) 127.
- [8] J.-D. Kim, Y.-I. Park, K. Kobayashi, M. Nagai, M. Kunimatsu, Solid State Ionics 140 (2001) 313.
- [9] B. Müller, N. Wagner, W. Schnurnberger, in: S. Gottesfeld, T.F. Fuller (Eds.), Proton Conducting Membrane Fuel Cells II, Electrochemical Society Proceedings, vol. 98-27, 1999, pp. 187–199.
- [10] C.A. Schiller, F. Richter, E. Gülzow, N. Wagner, Phys. Chem. Chem. Phys. 3 (2001) 374.
- [11] W. Ehm, H. Göhr, R. Kaus, B. Röseler, C.A. Schiller, Acta Chim. Hung. 137 (2000) 145.
- [12] N. Wagner, Thesis, University Erlangen-Nürnberg, 1989.
- [13] W. Ehm, H. Göhr, R. Kaus, B. Röseler, C.A. Schiller, Models Chem. 137 (2000) 145.
- [14] B. Müller, VDI-Berichte, Reihe 6, Nr. 466, 2001.
- [15] Thales/IM6 Manual, Zahner, Kronach, Germany.
- [16] N. Wagner, M. Schulze, Electrochim. Acta, in press.
- [17] B. Savova-Stoynov, Z. Stoynov, Computer analysis of non-stationary impedance data, in: M.W. Kendig, U. Bertocci, J.E. Strutt (Eds.), Proceedings of the Symposium on Computer Aided Acquisition and Analysis of Corrosion Data, vol. 85-3, The Electrochemical Society, Pennington, 1985, pp. 152–158.
- [18] Z. Stoynov, Electrochim. Acta 35 (1990) 1493.
- [19] B. Savova-Stoynov, Z.B. Stoynov, Electrochim. Acta 37 (1992) 2353.
- [20] Z. Stoynov, Electrochim. Acta 38 (1993) 1919.
- [21] N. Wagner, J. Appl. Electrochem., in press.
- [22] C.A. Schiller, F. Richter, E. Gülzow, N. Wagner, Phys. Chem. Chem. Phys. 3 (2001) 2113.
- [23] H. Gohr, Electrochem. Appl., vol. 1, 1997 (Available from <http://www.zahner.de>).
- [24] H. Göhr, Ber. Bunsenges. Phys. Chem. 85 (1981) 274.
- [25] X. Wang, I.-M. Hsing, Y.-J. Leng, P.-L. Yue, Electrochim. Acta 46 (2001) 4397.
- [26] N. Wagner, J. Appl. Electrochem. 32 (2002) 859.
- [27] R.J. Bellows, E.P. Maruchchi-Soos, D. Buckley, Analysis of reaction kinetics for carbon monoxide and carbon dioxide on polycrystalline relative to fuel cell operation, Ind. Engl. Chem. Res. 35 (1996) 1235.